Dynamics of Information Erasure and Extension of Landauer's Bound to Fast Processes

Salambô Dago and Ludovic Bellon*
Univ Lyon, ENS de Lyon, CNRS, Laboratoire de Physique, F-69342 Lyon, France

(Received 8 October 2021; accepted 31 January 2022; published 17 February 2022)

Using a double-well potential as a physical memory, we study with experiments and numerical simulations the energy exchanges during erasure processes, and model quantitatively the cost of fast operation. Within the stochastic thermodynamics framework we find the origins of the overhead to Landauer's bound required for fast operations: in the overdamped regime this term mainly comes from the dissipation, while in the underdamped regime it stems from the heating of the memory. Indeed, the system is thermalized with its environment at all times during quasistatic protocols, but for fast ones, the inefficient heat transfer to the thermostat is delayed with respect to the work influx, resulting in a transient temperature rise. The warming, quantitatively described by a comprehensive statistical physics description of the erasure process, is noticeable on both the kinetic and potential energy: they no longer comply with equipartition. The mean work and heat to erase the information therefore increase accordingly. They are both bounded by an effective Landauer's limit $k_B T_{\mathrm{eff}} \ln 2$, where T_{eff} is a weighted average of the actual temperature of the memory during the process.

DOI: 10.1103/PhysRevLett.128.070604

Information processing in the physical world comes with an energetic cost: erasing a 1-bit memory at temperature T_0 requires at least $k_B T_0 \ln 2$ of work, as demonstrated theoretically [1] and experimentally [2–10], with k_B Boltzmann's constant. Practical implementations require an overhead to Landauer's bound (LB), observed to scale as $k_B T_0 \times B/\tau$, with τ the protocol duration and B close to the system relaxation time [7]. Most experiments use overdamped systems, for which minimizing the overhead means minimizing the dissipation. Underdamped systems [10–12] therefore seem natural to reduce this energetic cost. But cutting the dissipative energy cost has a counterpart: in this Letter, we show experimentally and theoretically that, for such systems, fast erasures induce a heating of the memory and an accordingly higher energy expense, $k_B T_{\mathrm{eff}} \ln 2$. The work influx is indeed not instantaneously compensated by the inefficient heat transfer to the thermostat, which results in a transient temperature rise visible in the kinetic and potential energy evolutions. Our model covering all damping regimes paves the way to new optimization strategies [13], based on the thorough understanding of the energy exchanges.

The system under scrutiny is illustrated in Fig. 1: an underdamped micromechanical oscillator confined in a double-well potential $U_1(x, x_1) = \frac{1}{2} k(|x| - x_1)^2$, with x the position of the oscillator, k its stiffness, and x_1 the user-controlled parameter tuning the barrier height [10]. In our study, the only relevant degree of freedom of the physical system, a microcantilever, is its first deflection mode. The 1-bit information is encoded in the mean position: using a large barrier ($x_1 = X_1 \gg \sigma_0 = \sqrt{k_B T_0/k}$), the system can be at equilibrium either in the state 0 (in the left-hand well centered in $-X_1$) or in the state 1 (in the right-hand well centered in $+X_1$). The erasure process (illustrated in the Supplemental Material [14]) consists in lowering the barrier and merging the wells (stage 1: decreasing x_1 from X_1 to 0 in a time τ), then translating the single well $U_2(x, x_1) = \frac{1}{2} k(x + x_1)^2$ to position $-X_1$ (stage 2: increasing x_1 from 0 to X_1 in a time τ), before recreating the second well centered in $+X_1$ to recover the initial potential U_1 [10]. The experimental probability distribution function (PDF) evolution in gray on Fig. 1(c) points out the 100% success rate: this protocol always drives the system in state 0 independently of its initial state.

Along a trajectory, the total energy of the system consists in the sum of the potential energy U and of the kinetic energy $K = \frac{1}{2} m v^2$ (with m the oscillator mass and $v = \dot{x}$ its speed): $E = U + K$. This quantity equilibrates with the stochastic work $\mathcal{W}$ and heat $\mathcal{Q}$ through the energy balance equation

$$\frac{dE}{dt} = \frac{dU}{dt} + \frac{dK}{dt} = \frac{d\mathcal{W}}{dt} - \frac{d\mathcal{Q}}{dt}. \tag{1}$$

This energy balance is the starting point of the model developed in this Letter to explain the heating of the memory during erasure, using an approach similar to that followed in the theoretical description of feedback cooling [11,12].

The data plotted in Fig. 1(c) (x and x_1 along a trajectory) contains all we need to compute the quantities involved in Eq. (1). Indeed, applying to the underdamped regime the

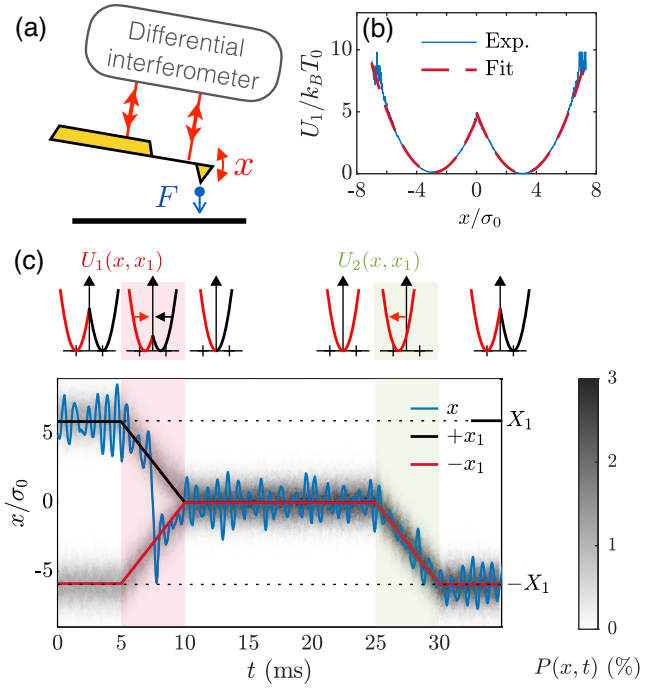

FIG. 1. Experimental setup and fast erasure cycle. (a) Schematic diagram of the experiment: the underdamped oscillator (resonance frequency $f_0 = \omega_0/(2\pi) = 1270$ Hz, quality factor $Q = 10$) is a conductive cantilever, sketched in yellow. Its deflection x is measured with a differential interferometer [18]. The potential U is created by the electrostatic force F between the cantilever and the electrode facing it [10]. (b) Measured double-well potential energy U_1 (blue) when $x_1 = \sqrt{10}\sigma_0$ ($5k_BT_0$ barrier height), with $T_0 = 295$ K and $\sigma_0 = \sqrt{k_BT_0/k} \sim 1$ nm, the standard deviation of the deflection at equilibrium inside a single well. The potential is inferred from the measured PDF of x during a 10 s acquisition and the Boltzmann distribution. The fit to the $U_1(x, x_1)$ expression is excellent (dashed line). (c) Time recording of the cantilever deflection x on a single trajectory (blue, starting in state 1 in this example), superposed with the centers of two wells: $+x_1$ (black) and $-x_1$ (red). Snippets of the potential energy on top of the plot sketch the erasure protocol. Stage 1 (red background) and 2 (green background) both last $\tau = 5$ ms. The equilibrium periods around stages 1 and 2 are chosen freely as long as they allow the cantilever to relax (natural relaxation time: $\tau_r = 2Q/\omega_0 \sim 2.5$ ms). The gray map corresponds to the PDF of x, computed from $N = 2000$ experimental trajectories of the erasure process.

generic computations of stochastic energy exchanges [10,19–24], we have

$$\frac{d\mathcal{W}}{dt} = \frac{\partial U}{\partial x_1}\dot{x}_1, \tag{2}$$

$$\frac{d\mathcal{Q}}{dt} = -\frac{\partial U}{\partial x}\dot{x} - \frac{dK}{dt}. \tag{3}$$

In Ref. [10] we measure the mean work and dissipated heat of erasure processes at different ramp speeds, starting from the quasistatic regime ($\tau f_0 = 250$), to very fast erasures [$\tau f_0 \sim 6$ in Fig. 1(c)]. As stated earlier, reducing the operation time requires an overhead to LB: the mean work and heat on an erasure cycle are, to a first approximation, $\langle\mathcal{W}\rangle = \langle\mathcal{Q}\rangle \sim k_BT_0(\ln 2 + B/\tau)$. In this Letter, we explain the origin of this overhead increasing with the speed: it comes in underdamped memories from the transient rise of the effective temperature T_{eff}, a source of energy loss that fundamentally differs from the viscous dissipation contribution of overdamped systems.

For this purpose, we measure the mean kinetic and potential energy during either a quasistatic erasure [Figs. 2(a) and 2(b)] or a fast one [Figs. 2(c) and 2(d)]. When we proceed in a quasistatic fashion, the mean kinetic energy stays as expected at its equilibrium value $\frac{1}{2}k_BT_0$, while odd evolution of the mean potential energy complies with equipartition for the biquadratic shape of U_1 as detailed in the Supplemental Material [14]. For fast operations, the energy profiles are completely different: in particular they strongly increase during stage 1, before relaxing during the equilibration step. K can be decomposed into $\langle K\rangle = \frac{1}{2}m(\langle v\rangle^2 + \sigma_v^2)$, summing the contribution of the velocity mean value $\langle v\rangle$ that reflects the response to the well motion, and the velocity variance σ_v^2 that defines the kinetic temperature (following Ref. [25]) of the first deflection mode: $T = m\sigma_v^2/k_B$. The first term is responsible for the transient

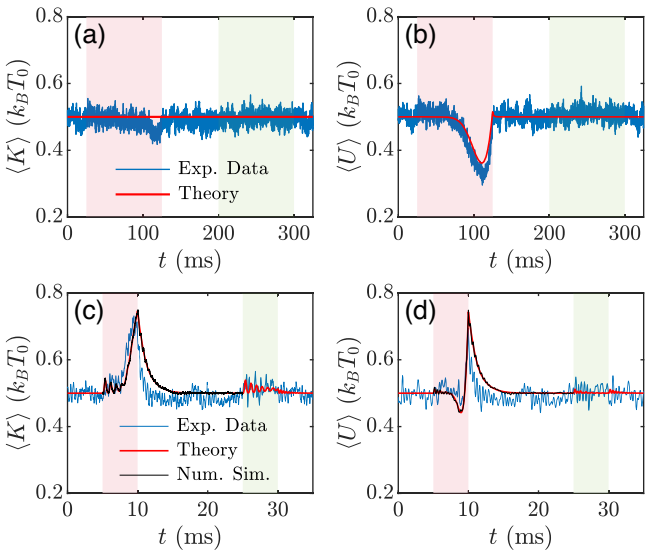

FIG. 2. Energy evolution during an erasure procedure. (a) In blue, the time evolution of the mean kinetic energy $\langle K\rangle$ in k_BT_0 units over $N = 2000$ iterations of a quasistatic erasure ($\tau f_0 \gg 1$): stage 1 and stage 2 (red and green backgrounds) both last $\tau = 100$ ms. The red line corresponds to the theoretical prediction detailed in the Letter. (b) Same, with the mean potential energy $\langle U\rangle$. (c),(d) Same for a fast erasure: $\tau = 5$ ms. We add in black line the results of a numerical simulation for step 1 that provides more samples than the experiment $N_{\text{sim}} = 5 \times 10^6$ and is thus free of statistical uncertainty.

oscillations at the beginning of step 1 and during step 2, but the energy rise during step 1 mainly comes from the thermal term: $\frac{1}{2}m\langle v\rangle^2 \sim \frac{1}{2}k_BT_0X_1^2/(2\pi\sigma_0\tau f_0)^2 \ll \frac{1}{2}k_BT_0$. It therefore demonstrates a transient temperature rise.

This warming and its consequences on the operation cost can be interpreted using a simple analogy: during step 1, the system behaves as a single-particle gas [26] at pressure p, compressed so that the available volume V is divided by 2. The infinitesimal work required for the compression is $d\mathcal{W}^c = -pdV = -k_BTd\ln V$. If the transformation is quasistatic, $T = T_0$ and the work simplifies into $\mathcal{W}^c = k_BT_0\ln 2$. In contrast, if the process is too fast to allow heat exchanges with the surrounding thermostat, the transformation is adiabatic, and the temperature T of the gas increases during the compression. Hence, the compression work for fast operations writes $\mathcal{W}^c = k_B\int_0^\tau Td\ln V = k_BT_{\rm eff}\ln 2$ with $T_{\rm eff} \geq T_0$. The heat exchanges after the adiabatic compression will then allow the system to thermalize at T_0.

By analogy, we will also call "compression" the reduction of the phase space volume explored when the bistable potential progressively shrinks until reaching a single well during step 1. This analogy highlights the fact that the warming during the compression is specific to the underdamped system and would not exist if a strong coupling to the bath allowed efficient heat exchanges. The objective of the following sections is to build a model that describes both the compression and translational motion as observed in experiment.

We first proceed with the mean dissipated heat described by [14]:

$$\frac{d\langle\mathcal{Q}\rangle}{dt} = \frac{\omega_0}{Q}[m\langle v\rangle^2 + k_B(T-T_0)]. \tag{4}$$

This expression is completely general and highlights that the heat exchanges are reduced at high quality factors Q.

To compute the other energetic terms ($\langle\mathcal{W}\rangle$, $\langle K\rangle$, and $\langle U\rangle$), we rely on the PDF of position x and speed v. Let us introduce this PDF during the compression stage, supposing that the system is at equilibrium: it is governed by the Boltzmann distribution

$$P^c(x,v) = \frac{1}{Z^c}e^{-\frac{1}{2}\beta mv^2}e^{-\frac{1}{2}\beta k(|x|-x_1)^2} \tag{5a}$$

$$Z^c(\beta,x_1) = \frac{2\pi}{\sqrt{km\beta}}V, \qquad V = 1+\mathrm{erf}\left(\sqrt{\frac{k\beta}{2}}x_1\right), \tag{5b}$$

with $\beta = 1/(k_BT)$, Z^c the partition function, and V a volumelike function that shrinks by a factor of 2 when x_1 decreases from X_1 to 0. We can directly apply this PDF to the slow erasures, in equilibrium at temperature T_0 at all times. We extend the use of this PDF to the case of fast erasures as well, under the hypotheses that (i) the cantilever oscillates several times in the double well before its shape changes significantly ($|\dot{x}_1| \ll \omega_0\sigma_0$), so that the phase space is adequately sampled and (ii) a Boltzmann-like distribution still holds. In this case, however, we leave the temperature T as a parameter free to evolve due to a possible heating. Note that the PDF $P^c(x,v)$ only describes the volume compression and does not include any transients, leaving aside any coupling between x and v. The main transient, due to the translational motion of the wells, is addressed in the next paragraph. In the Supplemental Material [14], we compare the PDF of our ansatz with one sampled on a large numerical simulation, demonstrating its relevancy.

During stage 2, or at the beginning of stage 1 before the oscillator crosses the barrier, the dynamics is ruled by a linear Langevin equation: the potential energy is quadratic (no switching). $x(t)$ is therefore the sum of the stochastic response to the thermal fluctuations, and of the deterministic response $\pm x_D(t)$ to the driving force $F_D(t) = \pm kx_1(t)$ (the sign depending on which well is considered). $x_D(t)$ can be easily computed for our simple $x_1(t)$ ramps, and the PDF $P^t(x,v)$, which determines the translational motion, is then described by [27,28]

$$P^t(x,v) = \frac{1}{Z^t}e^{-\frac{1}{2}\beta m(v-\dot{x}_D)^2}e^{-\frac{1}{2}\beta k(x-x_D)^2} \tag{6a}$$

$$Z^t = \frac{2\pi}{\sqrt{km\beta}}V, \qquad V = 1. \tag{6b}$$

We easily retrieve $\langle x\rangle = x_D$ and $\langle v\rangle = \dot{x}_D$.

In complement to Eq. (4) for the mean heat, having knowledge of the PDF allows the computation of all mean energetic quantities. During compression, for example, the mean energy is $\langle E^c\rangle = -\partial\ln Z^c/\partial\beta$, while the mean work derivative is $\langle\dot{\mathcal{W}}^c\rangle = \langle\partial U/\partial x_1\rangle\dot{x}_1 = -\dot{x}_1/\beta\partial\ln Z^c/\partial x_1$. In the Supplemental Material [14], we derive the following expressions, valid for all stages:

$$\frac{d\langle\mathcal{Q}\rangle}{dt} = \frac{\omega_0}{Q}(2K_D + k_BT - k_BT_0) \tag{7a}$$

$$\frac{d\langle\mathcal{W}\rangle}{dt} = \frac{d\mathcal{W}_D}{dt} - k_BT\frac{\partial\ln V}{\partial x_1}\dot{x}_1 \tag{7b}$$

$$\langle K\rangle = K_D + \frac{1}{2}k_BT \tag{7c}$$

$$\langle U\rangle = U_D + \frac{1}{2}k_BT + k_BT^2\frac{\partial\ln V}{\partial T}, \tag{7d}$$

where $\mathcal{W}_D$, K_D, and U_D are respectively the deterministic work and kinetic and potential energy that vanish in the quasistatic regime. With Eq. (7b) for a quasistatic compression in equilibrium at T_0, we recover the gas analogy $d\mathcal{W}^c = -k_BT_0d\ln V$; hence, LB: $\langle\mathcal{W}^c\rangle = k_BT_0\ln 2$.

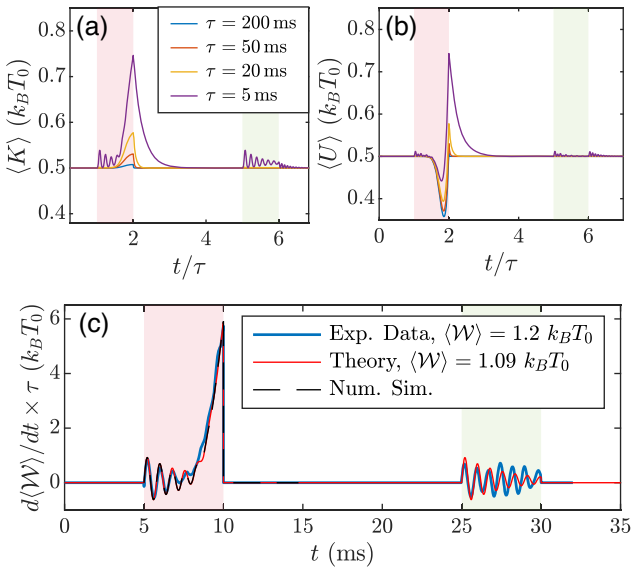

FIG. 3. Model prediction: energy and stochastic work profiles. (a) Time evolution of the mean kinetic energy $\langle K \rangle$ for different duration τ of the erasure steps computed from Eq. (7c). For small τ, $\langle K \rangle$ is affected during step 1 (red background) by a transient oscillation due to the dragging, followed by a strong rise in temperature. Only the dragging transient appears during step 2 (green background). (b) Same plot for the potential energy $\langle U \rangle$ from Eq. (7d). (c) Time evolution of the mean power over 2000 trajectories, following the fast protocol ($\tau = 5$ ms) corresponding to Fig. 1 (blue). The red line is computed using Eq. (7b) and closely matches the experimental results. Results of a numerical simulation (black dashed line), corresponding to 5×10^6 trajectories, match the model so well that we cannot distinguish the curves.

Using Eqs. (1) and (7), we derive a differential equation governing the time evolution of the temperature: the deterministic terms cancels out, since they obey the energy balance as well, and we are left with

$$\frac{d\langle E \rangle}{dt} = \frac{\partial \langle E \rangle}{\partial T}\dot{T} + \frac{\partial \langle E \rangle}{\partial x_1}\dot{x}_1 = -k_B T \frac{\partial \ln V}{\partial x_1}\dot{x}_1 + \frac{k_B \omega_0}{Q}(T - T_0). \tag{8}$$

Explicit formulas for $\partial\langle E \rangle/\partial T$ and $\partial\langle E \rangle/\partial x_1$ are readily computed from Eqs. (7c) and (7d). When we proceed in quasistatic fashion ($\dot{x}_1 \sim 0$), or when the volume is constant ($\partial/\partial x_1 = 0$), we observe no heating: $T = T_0$. For fast compressions, this equation can be solved numerically and leads to the evolution of the kinetic temperature $T(t)$.

Thanks to the knowledge of $T(t)$, our model describes the evolution of all energetic quantities in Eqs. (7a)–(7d) during the erasure process. For slow erasures, kinetic [Fig. 3(a)] and potential [Fig. 3(b)] energies comply as expected with equipartition. For fast erasures, we obtain a strong temperature increase [29] during step 1, visible on both energy profiles. The system then thermalizes before responding to the translational motion of step 2 with transient oscillations. Those theoretical results superimposed on Fig. 2 in red lines are in very good agreement with the experimental observations for both slow and fast erasures, with no adjustable parameters. We supplemented the model validation by numerical simulation data (see the Supplemental Material [14]): the black curve on Figs. 2(c) and 2(d) closely matches the model, except for tiny ripples during the thermalization that correspond to transients unaccounted for. Additionally, the model predicts that a fast erasure cycle will cause a mean power evolution that displays transient oscillations and a rise during compression, both of which are consistent with the experimental data of Fig. 3(c), and perfectly matches the simulation results.

All in all, we propose an efficient theoretical framework to predict the energy exchanges and explore the fast information erasure cost. The model only requires the system parameters (f_0 and Q) and the protocol ones (X_1 and τ) to estimate the erasure cost. As a further illustration of the model reliability, in Fig. 4 we compare its predictions with the experimental points and the empirical description of the overhead in B/τ: it successfully quantifies the divergence from LB as the speed is increased. The remaining difference may result from calibration drifts or experimental imperfections [30], or from the shortcomings of the model with respect to transients.

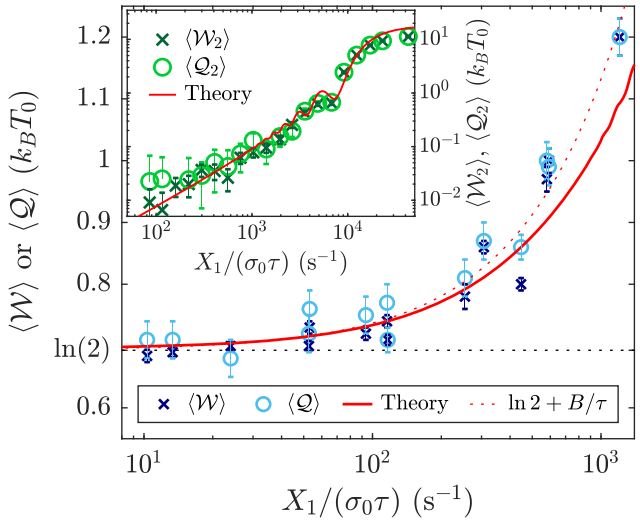

FIG. 4. Divergence from the Landauer limit for fast erasures. Erasure cost ($\langle \mathcal{W} \rangle$ and $\langle \mathcal{Q} \rangle$ in $k_B T_0$ units) for different operation speeds $X_1/(\sigma_0 \tau)$. Experimental data (in blue), computed from $N = 2000$ iterations each with $X_1 \sim 6\sigma_0$, are in good agreement with the analytical computation (red line). As a comparison, we plot the empirical description of the divergence from LB as $k_B T_0(\ln 2 + B/\tau)$ used in the existing literature, with $B = (2.6 \pm 0.2)$ ms here (red dotted line). Inset: same considering only the translational motion in step 2.

Furthermore, the model distinguishes the part of the overhead due to the compression from the one due to the translational motion. The latter, plotted in the inset of Fig. 4, behaves at first order as $X_1^2/(Q\omega_0)\tau s$ [7,10]. On the contrary, the former increases with the quality factor Q: it behaves as $k_B T_{\mathrm{eff}} \ln 2$, with $T_{\mathrm{eff}} > T_0$ the effective temperature during the process [14], rising when the heat exchanges with the bath are reduced (at high speeds or high Q). In the mean adiabatic limit (as defined in Ref. [25]) for erasure, however, the compression work saturates at $k_B T_0$ [14]. Indeed, for adiabatic transformations of underdamped systems, the conservation of the phase space volume [25] requires one to enslave the variations of the temperature T to those of the volume V. These considerations open several possibilities (that could be combined) to optimize the information processing: applying optimal protocols for the translational motion (predominant for overdamped systems) as suggested in Refs. [7,31,32]; moving to the underdamped regime to reduce the operation timescale and decrease the dragging cost [10], while paying only the adiabatic limit $k_B T_0$ for $Q \gg 1$.

As a conclusion, the underdamped framework addressed in this Letter opens up new possibilities in information processing: the operation times are several orders of magnitude smaller than the ones encountered in the overdamped regime, as is the cost required to move the system in the bath. Nevertheless, the price to pay to get rid of the viscous slowdown hides in the low coupling to the bath, allowing the memory temperature to strongly rise for fast drivings. We provide a full theoretical description of an erasure cycle, the results of which are verified by a wide panel of high-resolution experimental measurements and complementary numerical simulations. It culminates in the prediction of the overhead to LB for fast erasures. Such an understanding of the erasure process, covering all damping regimes, paves the way to new approaches to the information processing optimization.

This work has been financially supported by the Agence Nationale de la Recherche through Grant ANR-18-CE30-0013. We thank S. Ciliberto, J. Pereda and N. Barros for fruitful scientific discussions and advices.

Note added.—The data that support the findings of this study are openly available in Zenodo [33,34].

*Corresponding author.
ludovic.bellon@ens-lyon.fr

[1] R. Landauer, IBM J. Res. Dev. **5**, 183 (1961).
[2] A. Bérut, A. Arakelyan, A. Petrosyan, S. Ciliberto, R. Dillenschneider, and E. Lutz, Nature (London) **483**, 187 (2012).
[3] A. Bérut, A. Petrosyan, and S. Ciliberto, J. Stat. Mech. (2015) P06015.
[4] A. O. Orlov, C. S. Lent, C. C. Thorpe, G. P. Boechler, and G. L. Snider, Jpn. J. Appl. Phys. **51**, 06FE10 (2012).
[5] Y. Jun, M. Gavrilov, and J. Bechhoefer, Phys. Rev. Lett. **113**, 190601 (2014).
[6] M. Gavrilov and J. Bechhoefer, Europhys. Lett. **114**, 50002 (2016).
[7] K. Proesmans, J. Ehrich, and J. Bechhoefer, Phys. Rev. Lett. **125**, 100602 (2020).
[8] J. Hong, B. Lambson, S. Dhuey, and J. Bokor, Sci. Adv. **2**, e1501492 (2016).
[9] L. Martini, M. Pancaldi, M. Madami, P. Vavassori, G. Gubbiotti, S. Tacchi, F. Hartmann, M. Emmerling, S. Höfling, L. Worschech, and G. Carlotti, Nano Energy **19**, 108 (2016).
[10] S. Dago, J. Pereda, N. Barros, S. Ciliberto, and L. Bellon, Phys. Rev. Lett. **126**, 170601 (2021).
[11] J. Gieseler and J. Millen, Entropy **20**, 326 (2018).
[12] J. Gieseler, L. Novotny, C. Moritz, and C. Dellago, New J. Phys. **17**, 045011 (2015).
[13] A. Deshpande, M. Gopalkrishnan, T. E. Ouldridge, and N. S. Jones, Proc. R. Soc. A **473**, 20170117 (2017).
[14] See Supplemental Material, which includes Refs. [15–17], at http://link.aps.org/supplemental/10.1103/PhysRevLett.128.070604 for details on the erasure protocol, the experimental setup and the numerical simulation, the equipartition theorem applied to the bistable potential, the derivation of the theoretical predictions on work, heat, kinetic and potential energy, the validation of the PDF ansatz, the T_{eff} approximation, and the adiabatic limit of the information erasure cost.
[15] E. Hebestreit, Thermal Properties of Levitated Nanoparticles, Ph.D. thesis, ETH Zurich, 2017, Appendix A, https://www.research-collection.ethz.ch/handle/20.500.11850/250832.
[16] K. Burrage, P. Burrage, D. J. Higham, P. E. Kloeden, and E. Platen, Phys. Rev. E **74**, 068701 (2006).
[17] H. Kramers, Physica **7**, 284 (1940).
[18] P. Paolino, F. Aguilar Sandoval, and L. Bellon, Rev. Sci. Instrum. **84**, 095001 (2013).
[19] K. Sekimoto, *Stochastic Energetics*, Lecture Notes in Physics (Springer, New York, 2010), Vol. 799.
[20] K. Sekimoto and S. Sasa, J. Phys. Soc. Jpn. **66**, 3326 (1997).
[21] E. Aurell, K. Gawędzki, C. Mejía-Monasterio, R. Mohayaee, and P. Muratore-Ginanneschi, J. Stat. Phys. **147**, 487 (2012).
[22] U. Seifert, Rep. Prog. Phys. **75**, 126001 (2012).
[23] C. Jarzynski, Annu. Rev. Condens. Matter Phys. **2**, 329 (2011).
[24] S. Ciliberto, Phys. Rev. X **7**, 021051 (2017).
[25] I. A. Martinez, E. Roldan, L. Dinis, D. Petrov, and R. A. Rica, Phys. Rev. Lett. **114**, 120601 (2015).
[26] C. H. Bennett, Sci. Am. **257**, 108 (1987).
[27] A. Le Cunuder, I. A. Martínez, A. Petrosyan, D. Guéry-Odelin, E. Trizac, and S. Ciliberto, Appl. Phys. Lett. **109**, 113502 (2016).
[28] I. A. Martinez, E. Roldan, L. Dinis, D. Petrov, and R. A. Rica, Supplemental Material for Ref. [22] (2015).

[29] Since $\langle v\rangle^2 \ll \sigma_v$, $\langle K\rangle \sim \frac{1}{2}k_BT$ and the temperature profile can be read directly on the kinetic energy curve.
[30] S. Dago, J. Pereda, S. Ciliberto, and L. Bellon, arXiv:2201.09870.
[31] A. Gomez-Marin, T. Schmiedl, and U. Seifert, J. Chem. Phys. **129**, 024114 (2008).
[32] P. Geiger and C. Dellago, Phys. Rev. E **81**, 021127 (2010).
[33] S. Dago, J. Pereda, N. Barros, S. Ciliberto, and L. Bellon, 10.5281/zenodo.4626559 (2021).
[34] S. Dago and L. Bellon, 10.5281/zenodo.4807408 (2021).